NJC

Accepted Manuscript

This is an *Accepted Manuscript*, which has been through the Royal Society of Chemistry peer review process and has been accepted for publication.

Accepted Manuscripts are published online shortly after acceptance, before technical editing, formatting and proof reading. Using this free service, authors can make their results available to the community, in citable form, before we publish the edited article. We will replace this *Accepted Manuscript* with the edited and formatted *Advance Article* as soon as it is available.

You can find more information about *Accepted Manuscripts* in the Information for Authors.

Please note that technical editing may introduce minor changes to the text and/or graphics, which may alter content. The journal's standard Terms & Conditions and the Ethical guidelines still apply. In no event shall the Royal Society of Chemistry be held responsible for any errors or omissions in this *Accepted Manuscript* or any consequences arising from the use of any information it contains.

ROYAL SOCIETY OF CHEMISTRY

www.rsc.org/njc

NJC

PAPER

A novel cationic iridium(III) complex as red phosphor applied in warm white light-emitting diodes

Received 00th January 20xx,
Accepted 00th January 20xx

DOI: 10.1039/x0xx00000x

www.rsc.org/

Guoyun Meng, Zeyu Chen, Huaijun Tang,* Yong Liu, Liying Wei and Zhengliang Wang*

A novel red-emitting cationic iridium(III) complex [($\mathbf{L_m}$)$_2$Ir($\mathbf{L_a}$)]PF_6 ($\mathbf{L_m}$: 2-(9-(2-ethylhexyl)-9H-carbazol-3-yl)benzo[*d*]thiazole, $\mathbf{L_a}$: N,N-diphenyl-4-(5-(pyridin-2-yl)-1,3,4-oxadiazol-2-yl)aniline) was synthesized. Its ultraviolet-visible absorption and photoluminescent properties show the complex can be efficiently excited by 465 nm-emitting blue GaN chip, its decomposition temperature (T_d) is 340 °C, and its relative emission intensity at 100 °C is 88.3% of 25 °C. Perfect red light with a CIE value of (0.65, 0.34) was obtained when it was used as phosphor at 6.0 wt.% blending concentration in epoxy resin in blue GaN-based LED. A 465 nm-emitting blue GaN-based LED only using yellow-emitting $Y_3Al_5O_{12}:Ce^{3+}$ (YAG:Ce) as phosphor (1.0 wt.% in epoxy resin) emitted cold white, corresponding color rendering index (CRI) was 74.1, correlated color temperature (CCT) was 6026 K, and luminous efficiency (η_L) was 25.3 lm·W^{-1}. It became a neutral white light LED when the iridium(III) complex was added in at 0.5 wt.%, corresponding CRI was 79.5, CCT was 4004 K, and η_L was 32.6 lm·W^{-1}. It further became warm white LEDs when the complex was blended at 1.0 wt.% and 1.5 wt.%, corresponding CRI were 80.0 and 79.6, CCT were 3650 K and 3133 K, η_L were 25.5 lm·W^{-1} and 22.8 lm·W^{-1}, CIE values were (0.40, 0.39) and (0.43, 0.40) respectively. This complex is a promising red phosphor candidate for red LEDs and warm white LEDs.

1. Introduction

As the next generation solid-state light sources, white light-emitting diodes (WLEDs) have attracted intense attention and been developed rapidly, due to their potential applications in general illumination, full-color displays, liquid crystal display backlights, visible light communications (VLC), automobile headlights, optical detection in analytical instruments and so on.[1-7] Compared with conventional light sources (incandescent lamps and fluorescent lamps), WLEDs can provide some competitive advantages such as high efficiency, high brightness, low energy consumption, long lifetime and environment-friendly property.

White light emission can be achieved by several methods, such as the combinations of tricolor phosphors (blue, green and red) with UV-InGaN chips, double-color phosphors (green/yellow and red) with blue GaN chips, and one-color phosphors (yellow/orange) with blue GaN chips.[3,4,8,9] At present, the commercial WLEDs are mainly fabricated by the combination of blue LED chips and yellow-emitting $Y_3Al_5O_{12}:Ce^{3+}$ (YAG:Ce) phosphor.[3-5,7-12] However, because the main emission of the YAG:Ce is in the greenish yellow region, such WLEDs show low color rendering index (CRI) and high correlated color temperature (CCT) due to the lack of red light component in their spectra.[7, 13-17] There are mainly two approaches to overcome these drawbacks. In the first approach, some other metal ions (such as Cu^{+},[10] Eu^{3+},[13] Pr^{3+}.[14]) were doped in YAG:Ce for increasing red light component, although slightly red light was emitted by these optimized YAG:Ce, the yellow emission was obviously decreased. In the other approach, red phosphors were added in YAG:Ce based WLEDs,[15-18] comparatively, this is a better approach because better luminescent performances (such as CRI, CCT and efficiency) were obtained. Good red phosphors are very important and key in the second approach, up to now, numerous red phosphors (such as Ce^{3+}, Eu^{2+} or Mn^{4+} activated inorganic oxysalts, silicon nitrides, silicon oxynitrides, and thiosilicates,[15,18-23] quantum dots,[16,24-26] Mn^{4+} activated fluorides,[7,17,27] organic europium(III) complexes.[28-30]) have been developed for LEDs, however, perfectly satisfactory red phosphors for practical applications in WLEDs based on YAG:Ce and blue GaN chips are still very scarce due to various drawbacks and problems. These drawbacks and problems include too strong thermal quenching even at low temperature (such as $CaZnOS:Eu^{2+}$ and $Sr_2CeO_4:Eu^{3+}$)[19, 31], deep red and near-IR emission giving the low eye sensitivity (such as $Ca_{14}Al_{10}Zn_6O_{35}:Mn^{4+}$)[18], the excitation/absorption bands of red phosphors having poor overlaps with blue light emtting from GaN chips and therefore making them almost useless (such as organic europium(III) complexes)[28-30], potential degradation under high temperature and humidity conditions (such as $M_2SiO_4:Eu^{2+}$ (M = Ca^{2+}, Sr^{2+}, Ba^{2+}), $(Sr,Ca)_3Si_{1-x}Al_xO_{4+x}F_{1-x}:Ce^{3+}$ and $K_2SiF_6:Mn^{4+}$)[32], and so on.

At present, the most active and promising red phosphors systems such as semiconductor quantum dots (QDs)[16,24-26] and Mn^{4+} doped fluorides[7,17,27] are also beset with some drawbacks. Semiconductor QDs are capable to adjust the emission energy by utilizing the quantum size effect, and their emission light colors are tunable by changing the particle size of the nanocrystal during synthesis. The drawbacks of QDs include environmental concerns because of many bright emitting QD

Key Laboratory of Comprehensive Utilization of Mineral Resources in Ethnic Regions, Joint Research Centre for International Cross-border Ethnic Regions Biomass Clean Utilization in Yunnan, School of Chemistry & Environment, Yunnan Minzu University, Kunming 650500, China. *E-mail: tanghuaijun@sohu.com, wzhl629@163.com. Tel: 86-871-65913013*

† Electronic Supplementary Information (ESI) available: See
DOI: 10.1039/x0xx00000x

materials containing Cd^{2+},[24,25] the difficulties of accurate size control during synthesis and application, QDs absorption of the emission from other phosphors in the blend, thermal quenching and cost.[32] Mn^{4+} doped fluorides can be taken as improved products of Mn^{4+} doped oxysalts red materials. The emission of Mn^{4+} doped in oxysalts (such as Mg_2TiO_4:Mn^{4+} and $Ca_{14}Al_{10}Zn_6O_{35}$:Mn^{4+})[18, 33] is located in deep red region usually between 650 and 730 nm, which are too far red-shifted for efficient warm WLEDs with a high luminous efficiency.[7,17] However, Mn^{4+} doped in fluorides (such as K_2SiF_6:Mn^{4+} and $BaGeF_6$:Mn^{4+})[7,17,27] exhibit a "blueshift" of the $^2E \rightarrow {}^4A_2$ transition relative to oxide hosts, and the emission of them usually occurs between 590 and 660 nm. This blueshift is thought to be a result of the weakening of the nephelauxetic effect in highly ionic fluoride crystals which results in increased values of Racah parameters.[32] The narrow–red emission of Mn^{4+} doped fluorides between 590 and 660 nm can better match the eye sensitivity and are useful for lighting and display applications because higher CRI and efficacy can be obtained, at the same time, the thermal quenching in these materials is not significant at normal working temperature (below 150 ℃).[7,17,32] Although the advantages of Mn^{4+} doped fluorides are obvious, their drawbacks must be paid close attention. The drawbacks include a hazardous and corrosive chemical HF being used in the synthesis, and being susceptible to degradation under high temperature and humidity conditions due to the solubility in water and potential hydrolysis of Mn^{4+}-F^- bonds.[32] So it is still very important and urgent to develop new efficient red phosphors as additives for WLEDs.

Up to now, most of phosphors used in LEDs are inorganic down-conversion luminescent materials mainly due to their high stability and energy conversion efficiency.[34] At the same time, many organic down-conversion luminescent materials, such as organic rare earth complexes,[28-30] organic boron complexes,[35] organic iridium(III) complexes,[36-38] luminescent polymers[39,40] and small-molecule fluorescent dyes[40-42] also have been used as phosphors in LEDs and some other advantages such as broad emission spectra, good color tenability and hydrophobic nature without susceptibility to humidity have been exhibited. Organic cationic iridium(III) complexes luminescent materials were rapidly developed in the recent ten years and have been widely applied in light-emitting electrochemical cells (LECs)[43,44] and organic light-emitting diodes (OLEDs)[45-47] due to their high efficiency of 100% theoretical quantum efficiency, hydrophobic nature, broad emission and excellent color tunability via various ligands, high thermal and photic stability[43-47]. In this work, in order to develop new red phosphors, a novel red-emitting cationic iridium(III) complex was synthesized, characterized and used as red phosphor in YAG:Ce based WLEDs with 465 nm-emitting GaN blue chips.

2. Experimental section

2.1 Synthesis and characterization of the iridium(III) complex

2.1.1 General information

All chemicals and reagents were purchased from chemical reagent companies and used without further purification unless otherwise stated. ^{1}H NMR spectra were recorded on a Bruker AV400 spectrometer operating at 400 MHz, tetramethylsilane (TMS) was used as internal standard. Elemental analyses (EA) were performed on a Vario EL III Elemental Analysis Instrument. Mass spectra (MS) were obtained on a Bruker amaZon SL liquid chromatography mass spectrometer (LC-MS) with an electrospray ionization (ESI) interface using acetonitrile as matrix solvent. Ultraviolet-visible (UV-vis) absorption spectra were measured on an Agilent 8453 UV-visible Spectroscopy System. Photoluminescence (PL) spectra were recorded on a Jobin Yvon FL3-21 spectrofluorometer at room temperature and a 450 W xenon lamp was used as excitation source, and the temperature of solid sample was controlled by a temperature controller (REX-C110, Kaituo Compressor Parts Co. Ltd, Dongguan City, China). Thermogravimetry (TG) and differential thermal gravimetric (DTG) analysis curves were measured on a Netzsch STA449F3 thermal analyzer at a heating rate 10 ℃ min^{-1} under N_2. The electroluminescence of LEDs was recorded on a high accurate array spectrometer (HSP6000, HongPu Optoelectronics Technology Co. Ltd, Hangzhou City, China).

The synthetic route and chemical structure of the cationic iridium(III) complex are shown in Scheme 1, experimental details and characterization data are given in the following.

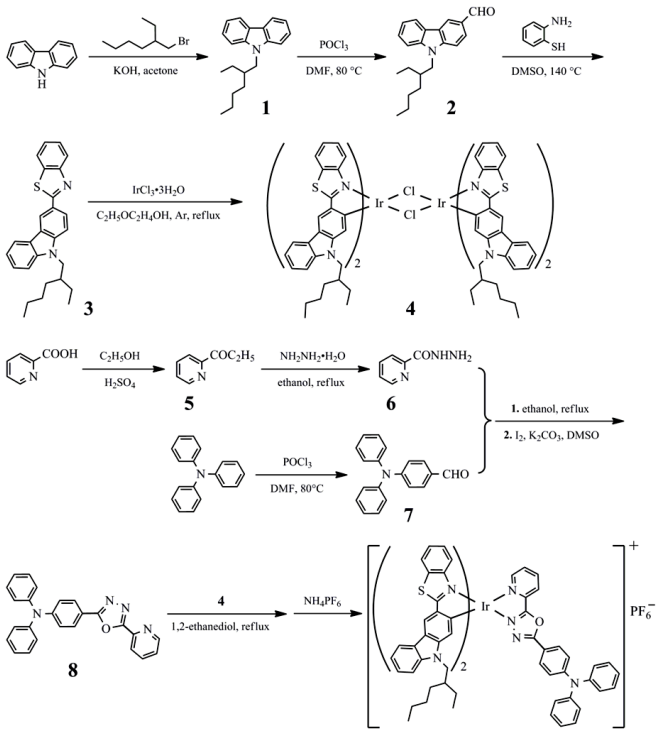

Scheme 1 Synthetic route and chemical structure of the iridium(III) complex.

2.1.2 Synthesis of 2-(9-(2-ethylhexyl)-9*H*-carbazol-3-yl)benzo[*d*]thiazole (3)

9-(2-ethylhexyl)-9H-carbazol (**1**) and 3-Foormyl-9-(2-ethylhexyl)-9H-carbazol (**2**) were synthesized according to the published procedure.[47] Compound **2** (2.3 g, 7.49 mmol) and 2-aminothiophenol (0.94 g, 7.52 mmol) were dissolved in dimethyl sulfoxide (DMSO, 20 mL). The mixture was stirred at 140 ℃ for 8 h, then poured into water and extracted with dichloromethane. The organic phase was washed with brine and dried by anhydrous $MgSO_4$. After the solvent being removed, the residue was purified by silica gel column chromatography using dichloromethane and hexane (volume rate, 1:1) as the eluent. Yield 68.2% (2.1 g), brownish-yellow oil. ^{1}H NMR (400MHz, $CDCl_3$, ppm), δ: 8.83 (d, 1H, ^3J = 1.6 Hz, ArH), δ:

8.15–8.20 (m, 2H, ArH), δ: 8.07 (d, 1H, ^3J = 8.0 Hz, ArH), δ: 7.89 (dd, 1H, ^3J = 8.0 Hz, ^4J = 0.4 Hz, ArH), δ: 7.24–7.50 (m, 6H, ArH), δ: 4.16 (dd, 2H, ^3J = 7.6 Hz, ^4J = 2.0 Hz, ^4J = 3.5 Hz, –N–CH_2–), δ: 2.01–2.11 (m, 1H, –CH<), δ: 1.26–1.39 (m, 8H, alkyl–H), δ: 0.91 (t, 3H, ^3J = 5.7 Hz, –CH_3), δ: 0.86 (t, 3H, ^3J = 4.4 Hz, –CH_3). Calc. for $C_{27}H_{28}N_2S$: C, 78.60; H, 6.84; N, 6.79 %. Found: C, 78.65; H, 6.65; N, 6.81 %.

2.1.3 Synthesis of the chloro-bridged dimer (4)

A mixture of $IrCl_3{\cdot}3H_2O$ (0.89 g, 2.5 mmol) and compound **3** (2.10 g, 5.10 mmol) in H_2O (8 mL) and 2-methoxyethanol (24 mL) was refluxed under argon for 24 h. After being cooled to room temperature, the resultant yellow precipitate was collected on a filter, washed with water and methanol alternately, then dried in vacuum. Yield 84.3% (2.20 g), yellow solid. This dimer product was directly used for the next step after being dried in vacuum without further purification and characterization.

2.1.4 Synthesis of N,N-diphenyl-4-(5-(pyridin-2-yl)-1,3,4-oxadiazol-2-yl)aniline (8)

1-(pyridine-2-yl)propan-1-one (**5**) and picolinohydrazide (**6**) were synthesized according to a procedure described in previous publications.[48] 4-(Diphenylamino)benzaldehyde (**7**) also was prepared according to the published procedures.[49] A solution of compound **6** (0.45 g, 3.28 mmol) and compound **7** (0.90 g, 3.28 mmol) in ethanol (10 mL) was refluxed under Ar atmosphere for 8 h, and then the solvent was removed by vacuum distillation. The resultant residue was redissolved in DMSO (10 mL), then potassium carbonate (1.37 g, 9.91 mmol) and iodine (1.2 g, 4.73 mmol) were added in. The mixture was stirred at 100 ℃ for 4 h. After being cooled to room temperature, a solution of $Na_2S_2O_3$ (5%) was droped in the reaction mixture until the brown disappeared, extracted with ethyl acetate (3 × 15 mL). The organic phase was washed with brine (3 × 10 mL) and dried by anhydrous Na_2SO_4. The solvent was distilled off and the residue was purified by silica gel column chromatography using a mixture of ethyl acetate and dichloromethane (volume rate, 1:20) as eluent to afford the desired compound **8**. Yield 62.5% (0.80 g), yellowish-green solid. ^{1}H NMR (400MHz, $CDCl_3$, ppm), δ: 8.80 (d, 1H, ^3J = 4.4 Hz, pyridine–H), δ: 8.30 (d, 1H, ^3J =8.0 Hz, ArH), δ: 8.02 (d, 2H, ^3J = 8.0 Hz, ArH), δ: 7.89(t, 1H, ^3J = 8.0 Hz, ArH), δ: 7.46 (t, 1H, ^3J = 6.4 Hz, ArH), δ: 7.32 (t, 4H, ^3J = 7.6 Hz, ArH), δ: 7.09-7.18 (m, 8H, ArH).

2.1.5 Synthesis of the iridium(III) complex

The chloro-bridged dimer **4** (0.68 g, 0.32 mmol) and compound **8** (0.25 g, 0.64 mmol) were added in 1, 2-ethanediol (30 mL). The mixture was heated to 150 ℃ and kept under argon atmosphere with stirring for 16h. After being cooled to room temperature, an orange solution was obtained, then 10 mL aqueous solution of NH_4PF_6 (1.0 mol·L^{-1}) was added, a yellow suspension appeared immediately. The solid was filtered, washed with water and dried in vacuum. The crude product was purified by column chromatography on silica gel, eluting with CH_2Cl_2/MeCN (volume rate, 10:1). Yield 80.0% (0.80 g), brownish red solid. ^{1}H NMR (400MHz, $CDCl_3$, ppm), δ: 8.60 (d, 1H, ^3J = 7.6 Hz, ArH), δ: 8.53 (s, 1H, ArH), 8.49 (s, 1H, ArH), δ: 8.40 (t, 1H, ^3J = 8.0 Hz, ArH), δ: 8.05 (q, 2H, ^3J = 8.0 Hz, ArH), δ: 7.87–7.95 (m, 5H, ArH), δ: 7.40 (t, 2H, ^3J = 7.6 Hz, ArH), δ: 7.29–7.35 (m, 7H, ArH), δ: 7.11–7.22 (m, 13H, ArH), δ: 6.99 (d, 2H, ^3J = 8.0 Hz, ArH), δ: 6.33–6.42 (m, 2H, ArH), δ: 6.01 (m, 1H, ArH), δ: 3.60 (dd, 4H, ^3J = 14.4 Hz, ^4J = 6.8 Hz, –N–CH_2–), δ: 1.25 (s, 2H, –CH<), δ: 0.86–1.05 (m, 16H, alkyl–H), δ: 0.72 (t, 6H, ^3J = 5.6 Hz, –CH_3), δ: 0.46-0.57 (m, 6H, –CH_3); ESI–MS(m/Z): 1405.4 $[M–PF_6]^+$; Anal. Calc. for $C_{78}H_{71}F_6IrN_8OPS_2$: C, 60.92; H, 4.65; N, 7.29 %. Found: C, 61.57; H, 4.86; N, 6.94 %.

2.2. Fabrication and measurements of LEDs

Two kinds of LEDs were fabricated and measured in this work, one kind is red LEDs only using the cationic iridium(III) complex as phosphor and the other kind is WLEDs using the cationic iridium(III) complex together with YAG:Ce as phosphors. In the case of red LEDs devices, the iridium(III) complex was blended in epoxy resin homogeneously at the concentrations of 1.0, 2.0, 3.0, 4.0, 5.0 and 6.0 wt.% and coated on the surface of 465 nm-emitting GaN chips until the reflective cavities just were filled up. The coated chips were dried and solidified at 150 ℃ for 1h. Then they were completely encapsulated with transparent epoxy resin which was poured in semispherical molds. The WLEDs were fabricated by the same procedure of the abovementioned red LEDs. In fabrication of WLEDs, YAG:Ce phosphor was blended in epoxy resin at a constant mass ratio of 1.0 wt.%, however, the iridium(III) complex phosphor was blended together at different mass ratios, those are 0.0, 0.5, 1.0 and 1.5 wt.%. The performances of all LEDs were measured by an integrating sphere spectroradiometer system (Everfine PMS-50). The LEDs were operated at 20 mA forward current and 5 V reverse voltage.

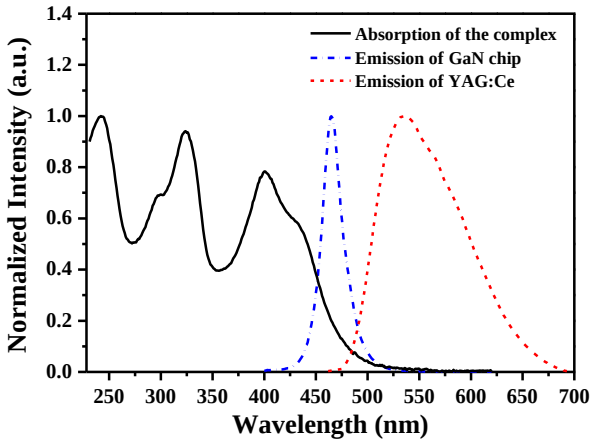

Fig. 1 Normalized UV-vis absorption spectrum of the cationic iridium(III) complex in CH_2Cl_2 solution at 1.0 × 10^{-5} mol·L^{-1} and emission spectra of blue GaN chip and YAG:Ce.

3. Results and discussion

3.1 UV–vis absorption spectrum

The UV–vis absorption spectrum of the cationic iridium(III) complex was measured in CH_2Cl_2 solution at room temperature and the result together with emission spectra of blue GaN chip and YAG:Ce are shown in Fig. 1. There are three strong peaks on the absorption spectrum, the corresponding maximum absorption wavelengths ($\lambda_{abs,\ max}$) are 242 nm (ε_{242nm} = 6.79 × 10^4 L mol^{-1} cm^{-1}), 324 nm (ε_{324nm} = 6.28 × 10^4 L mol^{-1} cm^{-1}) and 401 nm (ε_{401nm} = 5.20 × 10^4 L mol^{-1} cm^{-1}), such strong

absorption bands are mainly caused by the spin-allowed $^1\pi$-π^* transition in the ligands.[50] The relatively weak absorption bands at longer wavelength region (about 420–565 nm) can be attributed to an admixture of the spin-allowed singlet metal-to-ligand charge-transfer (^{1}MLCT) and spin-forbidden triplet metal-to-ligand charge-transfer (^{3}MLCT) and $^3\pi$-π^* in the ligands.[50,51] The admixture absorption of ^{3}MLCT and $^3\pi$-π^* with higher-lying ^{1}MLCT is caused by the strong spin-orbit coupling induced by the heavy iridium atom.[51] As shown in Fig. 1, there is large overlap between the absorption spectrum of the iridium(III) complex and emission spectrum of blue GaN chip ($\lambda_{em,\ max}$ = 465 nm) which suggests that Förster resonance energy transfer (FRET) is able to happen between them easily and this iridium(III) complex can be well excited by the blue GaN chip.[52] On the contrary, the overlap between the absorption spectrum of the iridium(III) complex and the emission spectrum of YAG:Ce is very limited, so the emission of YAG:Ce almost would not be affected by the iridium(III) complex and such iridium(III) complex is a practicable red luminescent additive for YAG:Ce based WLEDs.

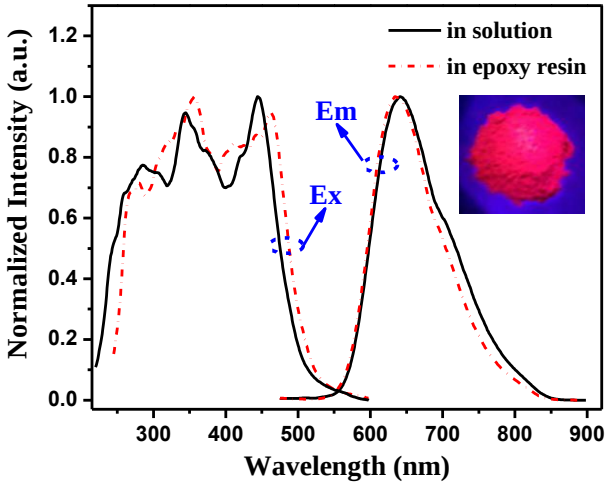

Fig. 2 Normalized excitation (Ex, λ_{em} = 639 nm) and emission (Em, λ_{ex} = 465 nm) spectra of the cationic iridium(III) complex in CH_2Cl_2 solution at 1.0 × 10^{-5} mol·L^{-1} and blended in epoxy resin at 6.0 wt.% (coated on quartz plate). Inset: a photograph of the iridium(III) complex powders excited by blue light (λ_{ex} = 465 nm).

3.2 Photoluminescent property

Normalized excitation (Ex, λ_{em} = 639 nm) and emission (Em, λ_{ex} = 465 nm) spectra of the cationic iridium(III) complex in CH_2Cl_2 solution at 1.0 × 10^{-5} mol·L^{-1} and blended in epoxy resin at 6.0 wt.% are shown in Fig. 2. Both the excitation and emission spectra of the cationic iridium(III) complex in CH_2Cl_2 solution and blended in epoxy resin are very similar to each other which suggests the conjugated systems of the complex in epoxy resin almost do not enlarge probably due to no palpable molecular interaction and π-π piles at low blending concentration. In general, sufficient overlap between excitation spectra of phosphors and emission spectra of the LED chips is very necessary to realize energy transfer from the LED chips to phosphors efficiently. In this work, the excitation spectra of the cationic iridium(III) complex in CH_2Cl_2 solution and blended in epoxy resin both lie from 245 nm to 510 nm, and both cover up the emission spectra of the 465-emitting blue GaN chip (as shown in Fig. 1) which means this cationic iridium(III) complex can be efficiently excited by the blue GaN chip. At the same time, the overlaps between the excitation spectra of the iridium(III) complex and the emission spectrum of YAG:Ce (as shown in Fig. 1) are still very limited which again demonstrates the emission of YAG:Ce almost would not be affected by the iridium(III) complex and both of them can be efficiently excited by the blue GaN chip. The emission spectra of the cationic iridium(III) complex mainly lie from 550 nm to 840 nm with the maximum emission wavelengths of 641 nm (in solution) and 635 nm (in epoxy resin) respectively, it is a perfect red phosphor.

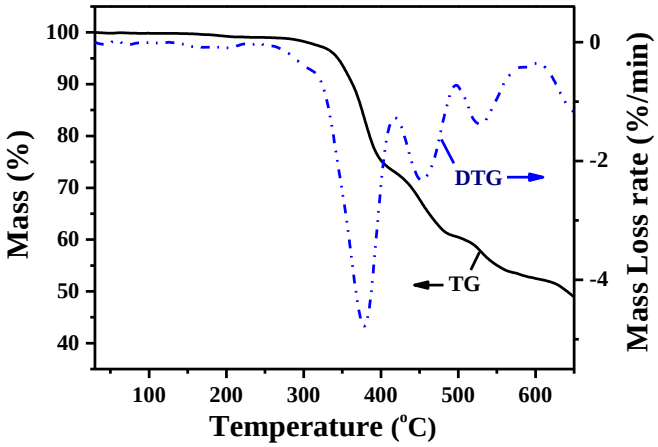

Fig. 3 TG and DTG curves of the iridium(III) complex.

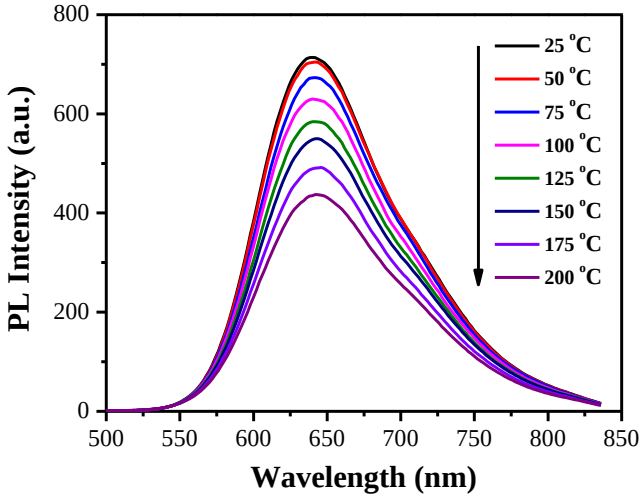

Fig. 4 The temperature-dependent PL spectra (λ_{ex} = 465 nm) of the cationic iridium(III) complex measured with increasing temperature from 25 °C to 200 °C.

3.3 Thermal stability and thermal quenching properties

Inorganic luminescent materials usually are synthesized by two ways: high temperature solid-state reaction (such as YAG:Ce) and solution-based chemical synthesis (such as Mn^{4+} doped fluorides).[34] The thermal stability of the inorganic luminescent materials prepared by solid-state reaction do not need to be additionally investigated, because the materials already have encountered high temperature in synthesis. However, the

thermal stability of organic luminescent materials must been studied due to exothermic working process of the LEDs and heat treatment in the device making.

The thermal stability of the cationic iridium(III) complex was investigated by TG and DTG under nitrogen atmosphere, the results are shown in Fig. 3. A tiny mass loss (about 1.0%) occurred on TG curve between 150 ~ 210 ℃ owing to the loss of adsorptive water and organic solvent residues. With temperature increasing, the TG curve begins to dip suddenly down after about 340 ℃ which means the thermal decomposition happened and 340 ℃ was its thermal decomposition temperature (T_d). From 210 ℃ to 405 ℃, a big mass loss of 24.6% happened mainly due to the loss of the neutral auxiliary ligand N,N-diphenyl-4-(5-(pyridine-2-yl)-1,3,4-oxadiazol-2-yl)aniline because the coordination bond is the weakest bond in such heteroleptic complexes.[47] Then anionic main ligand (9-(2-ethylhexyl)-9H-carbazol-3-yl) benzo[*d*]thiazole began to lose and decompose. Such high decomposition temperature (T_d = 340 ℃) of the iridium(III) complex suggests it have high thermal stability and is enough to meet the requirement of its application in LEDs, since LEDs devices are fabricated and work usually at a temperature below 150 ℃.[30]

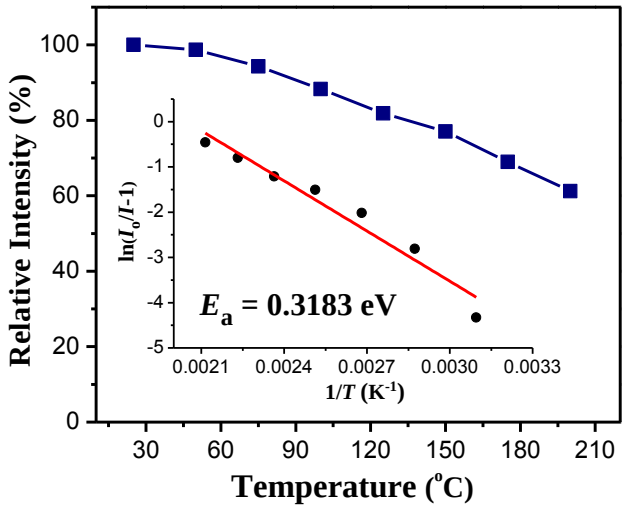

Fig. 5 The relative PL intensity of the cationic iridium(III) complex as a function of temperature. The inset represents the ln(I_o/I−1) versus 1/T and the calculated activation energy (Ea) for the cationic iridium(III) complex.

The thermal quenching properties of the iridium(III) complex were also investigated. Fig. 4 depicts the temperature-dependent PL spectra (λ_{ex} = 465 nm) of the cationic iridium(III) complex. The relative PL intensity of the cationic iridium(III) complex as a function of temperature is shown in Fig. 5. From 25 ℃ to 200 ℃, the profile, wavelength band and the maximum wavelengths (641 nm) of the emission spectra at different temperatures almost have not changed except the intensity, which suggests the light-emitting color of the iridium(III) complex itself have high thermal stability. Like most phosphors used in LEDs, the emission intensity of the iridium(III) complex decreases with increasing temperature (i.e. thermal quenching).[4,32] The relative PL intensities at different temperatures are (in descending order): 100% (at 25 ℃), 98.7% (at 50 ℃), 94.3% (at 75 ℃), 88.3% (at 100 ℃), 81.8% (at 125 ℃), 77.1% (at 150 ℃), 69.0% (at 175 ℃), 61.2% (at 200 ℃). The activation energy (E_a) of the thermal quenching can be described by the Arrhenius equation:[18,20,23]

$$I = \frac{I_o}{1 + A\exp(-\frac{E_a}{k_B T})}$$

where I and I_o represent the PL intensity of the iridium(III) complex at the experimental temperature and room temperature (RT, 25 ℃), A is a constant, and k_B is Boltzmann's constant. From the Arrhenius equation, the relationship of ln(I_o/I-1) with 1/T can be obtained, the experimental data are well-fitted and shown in Fig. 5 (inset), then E_a can be calculated by the slope value of −(E_a/k_B), the calculated value of E_a is 0.3183 eV. For different phosphors, higher E_a value means lower thermal quenching in a same range of rising temperature. Although the PL intensity decay rate and E_a value of the iridium(III) complex show its thermal quenching is greater than that of some red phosphors, mainly including some Eu^{2+} activated silicon nitrides[15], Mn^{4+} activated oxysalts and fluorides,[7,17,18] yet its thermal quenching is much lower than many red phosphors reported recently.[19,23,31,32] The result indicates that the iridium(III) complex has the potential as a red phosphor for WLEDs applications.

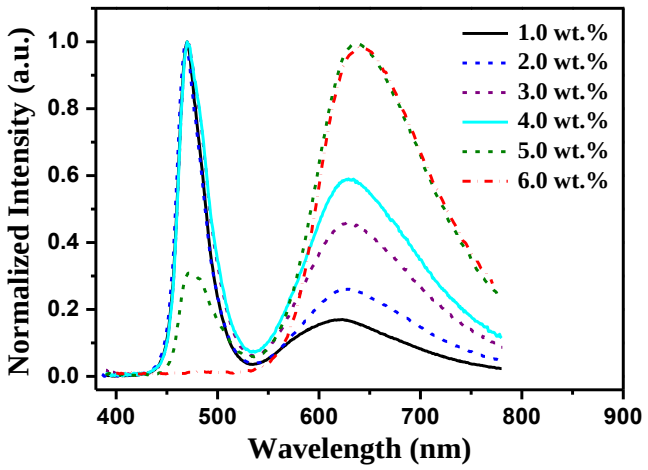

Fig. 6 Emission spectra of the blue GaN-based LEDs only using the cationic iridium(III) complex as phosphor at different blending concentrations at 20 mA forward current.

3.4 Performances of the LEDs

The luminescent property of GaN-based LEDs only using the cationic iridium(III) complex as phosphor was investigated at first. The emission spectra of the LEDs using the complex as phosphor blended in epoxy resin at different concentrations at 20 mA forward current are shown in Fig. 6, and the detailed performances are summarized in Table 1. The sharp blue emission peaks with the maximum wavelengths around 469 nm obviously originate from the emission of blue GaN chips. The broad emission bands from 560 nm to 780 nm with the maximum peaks around 630 nm can be ascribed to the emission of the cationic iridium(III) complex because they are primarily consistent with its PL spectra. With the increasing of the blending concentrations, the emission peaks of GaN chip gradually decline and eventually disappear at 6.0 wt.%, on the contrary, the emission peaks of the cationic iridium(III) complex gradually grow up. With the change of blending concentrations, the CIE (Commission Internationale de

L'Eclairage) chromaticity coordinates of the LEDs gradually moved from cold white light region to red light region. At 6.0 wt.%, only pure red light of the complex was emitted, a relatively high CRI of 71.9 and a low CCT of 1010 K were achieved, the CIE became (0.65, 0.34) which was very close to the "ideal red" value (0.67, 0.33) of NTSC (National Television Standard Committee). These results show the cationic iridium(III) complex is a potential red phosphor for improving the quality of YAG:Ce based WLEDs via increasing CRI and lowering CCT.

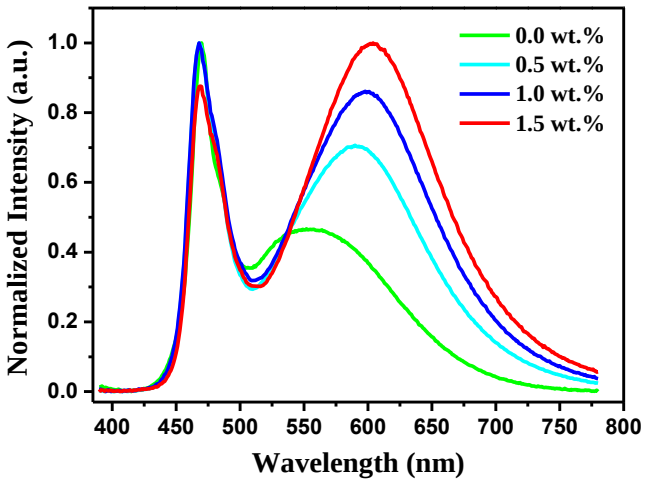

Fig. 7 Emission spectra of the blue GaN-based WLEDs using YAG:Ce (1.0 wt.%) and the cationic iridium(III) complex (*x* wt.%, *x* = 0.0, 0.5, 1.0, 1.5) as phosphors blended in epoxy resin at different concentrations.

To demonstrate the application of the cationic iridium(III) complex for WLEDs, a series of blue GaN-based WLEDs were fabricated by using YAG:Ce (1.0 wt.%) and the cationic iridium(III) complex (*x* wt.%, *x* = 0.0, 0.5, 1.0, 1.5) as phosphors blended in epoxy resin at different concentrations. The emission spectra of these WLEDs are shown in Fig. 7 and the performances of them are listed in the Table 2. It can be seen that the emission peaks on the right show obvious red-shift after the cationic iridium(III) complex being blended in, at the same time, the red-shift is positively related to the blending concentration, the maximum emission wavelengths ($\lambda_{em,\ max}$) of these peaks change from 552 nm to 593nm, then successively to 598 nm and 604nm. Moreover, the intensity of the emission peaks on the right increase with the increase of the blending concentrations, because the blending concentration of YAG:Ce is constant, so the increase of the emission intensity inevitably is caused by the increase of the cationic iridium(III) complex. With the red-shift of the emission peaks on the right, the CRI of the devices are improved, and the CCT are lowered. The broad red emission of the cationic iridium(III) complex is distinctly different from the sharp red emission of organic europium(III) complexes[28-30] and some inorganic salts doped with rare-earth ions or transition metals ions[17,27,31,34], the cationic iridium(III) complex can improve the red light component for WLEDs more effectively due to more complete red spectral band being contained. In this work, three YAG:Ce based WLEDs using the cationic iridium(III) complex as red phosphor (No. h, i and j as listed in the Table 2) all have exhibited high CRI (79.5, 80 and 79.6) and low CCT (4004 K, 3650 K and 3133 K). Compared with the performances of YAG:Ce based WLED without the cationic iridium(III) complex (No. g, CRI is 74, CCT is 6026K and η_L is 25.3 lm·W^{-1}), the total qualities of No. h, i, j have been improved significantly and warmer white lights are obtained. Such improvements also can be seen from the change of their CIE chromaticity coordinates as shown in Fig.8, with the increase of blending concentrations, the coordinate positions of the WLEDs in CIE chromaticity diagram move from cold white light region to neutral white light region, and then to warm white light region. Furthermore, such improvements also can be shown visually by their working state photographs, such as cold WLED (No. g), neutral WLED (No. h) and warm WLED (No. j) in Fig. 8, a working state photograph of the red LED (No. f) only using the cationic iridium(III) complex as phosphor at 6.0 wt.% also is shown in Fig. 8 as a reference object. Better performances should be obtained if the above-mentioned WLEDs were further optimized.

Table 1 Performances of the blue GaN-based LEDs only using the cationic iridium (III) complex as phosphor at different blending concentrations [a].

No. of LEDs	blending concentration (wt.%)	luminous efficiency (lm·W^{-1})	CRI	CCT (K)	$\lambda_{em,\ max}$ (nm)	CIE (*x*, *y*)
a	1.0	7.8	8.3	100000	470, 623	(0.26, 0.22)
b	2.0	5.2	10.6	19641	468, 628	(0.29, 0.22)
c	3.0	4.3	24.2	3984	470, 627	(0.35, 0.27)
d	4.0	3.6	30.6	2925	470, 629	(0.38, 0.29)
e	5.0	2.4	62.9	1490	471, 638	(0.54, 0.34)
f	6.0	1.0	71.9	1010	641	(0.65, 0.34)

[a] At 20 mA forward current and 5 V reverse voltage.

4. Conclusions

A novel red-emitting cationic iridium(III) complex was synthesized, its UV-vis absorption and PL properties showed it can be efficiently excited by 465 nm-emitting blue GaN chip, however, the emission of YAG:Ce almost would not be affected by it. It have high thermal stability with a decomposition temperature (T_d) of 340 ℃, and its relative emission intensity at 100 ℃ is 88.3% of 25 ℃. This cationic iridium(III) complex can effectively improve the red light

component for WLEDs, cold white GaN-based LED only using YAG:Ce (at 1.0 wt.%) can become neutral white LEDs when the complex was blended in epoxy resin at low concentrations (such as 0.5 wt.%), and can further become warm white LEDs with the increase of the blending concentrations (such as 1.0 wt.%, 1.5 wt.%). This cationic iridium(III) complex is a promising red phosphor candidate for red LEDs and warm white LEDs.

Table 2 Performances of the blue GaN-based WLEDs using YAG:Ce and the cationic iridium(III) complex as phosphors at different blending concentrations [a].

No. of LEDs	blending concentration (wt.%)		luminous efficiency ($lm \cdot W^{-1}$)	CRI	CCT (K)	$\lambda_{em,\ max}$ (nm)	CIE (x, y)
	YAG:Ce	complex					
g	1.0	0.0	25.3	74.1	6026	470, 552	(0.32, 0.38)
h	1.0	0.5	32.6	79.5	4004	468, 593	(0.38, 0.38)
i	1.0	1.0	25.5	80.0	3650	468, 598	(0.40, 0.39)
j	1.0	1.5	22.8	79.6	3133	469, 604	(0.43, 0.40)

[a] At 20 mA forward current and 5 V reverse voltage

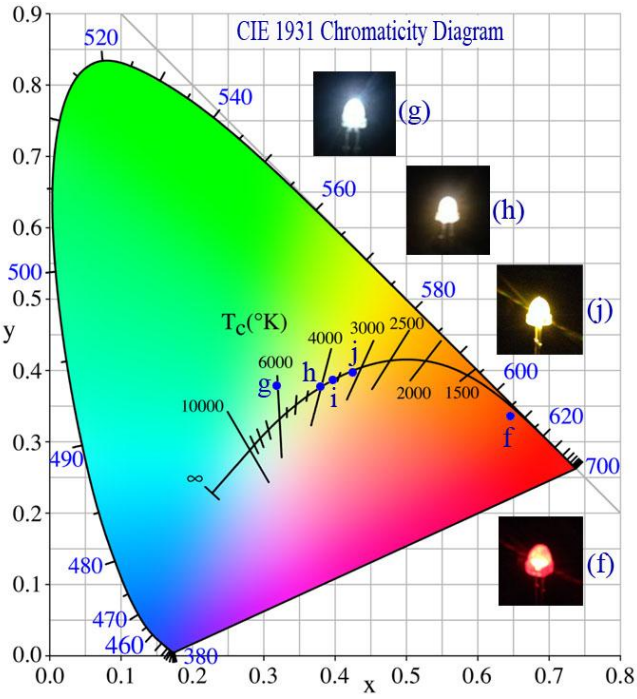

Fig. 8 CIE chromaticity coordinates of the blue GaN-based LEDs using YAG:Ce and the cationic iridium(III) complex as phosphors at different blending concentrations. (f) only 6.0 wt.% complex; (g) only 1.0 wt.% YAG:Ce; (h) 1.0 wt.% YAG:Ce and 0.5 wt.% complex; (i) 1.0 wt.% YAG:Ce and 1.0 wt.% complex; (j) 1.0 wt.% YAG:Ce and 1.5 wt.% complex. Inset: The photographs of the LEDs (g), (h), (j) and (f) in working state.

Acknowledgements

This work was supported by National Nature Science Foundation of China (No. 21262046 and 21261027), Key Scientific Research Fund of Yunnan Province Education Department (No. 2011Z003), and Innovation Program for postgraduate of Yunnan Minzu University (No. 2015YJCXXY263).

References

1 J. Y. Tsao, M. H. Crawford, M. E. Coltrin, A. J. Fischer, D. D. Koleske, G. S. Subramania, G. T. Wang, J. J. Wierer, R. F. Karlicek Jr., *Adv. Opt. Mater.*, 2014, **2(9)**, 809−836.
2 D. F. Feezell, J. S. Speck, S. P. DenBaars, S. Nakamura, *J. Disp. Technol.*, 2013, **9(4)**, 190−198.
3 E. F. Schubert, J. K. Kim, *Science*, 2005, **308(5726)**, 1274−1278.
4 L. Chen, C. C. Lin, C. W. Yeh, R S. Liu, *Materials*, 2010, **3(3)**, 2172−2195.
5 M. R. Krames, O. B. Shchekin, R. Mueller-Mach, G. O. Mueller, L. Zhou, G. Harbers, M. G. Craford, *J. Disp. Technol.*, 2007, **3(2)**: 160−175.
6 M. T. Sajjad, P. P. Manousiadis, H. Chun, D. A. Vithanage, S. Rajbhandari, A. L. Kanibolotsky, G. Faulkner, D. O'Brien, P. J. Skabara, I. D. W. Samuel, G. A. Turnbull, *ACS Photonics*, 2015, **2(2)**, 194−199.
7 H. Zhu, C. C. Lin, W. Luo, S. Shu, Z. Liu, Y. Liu, J. Kong, E. Ma, Y. Cao, R.-S. Liu, X. Chen, *Nature commun.*, 2014, **5**, 4312−1−10.
8 Y. Narukawa, I. Niki, K. Izuno, M. Yamada, Y. Murazaki, T. Mukai, *Jpn. J. Appl. Phys.*, 2002, **41(4A)**, L371−L373.
9 J. Dwivedi, P. Kumar, G. Kedawatc, B. K. Gupta, *New J. Chem.*, 2015, **39**, 5161−5170.
10 C. Zhao, D. Zhu, M. Ma, T. Han, M. Tu, *J. Alloys Compd.*, 2012, **523**, 151−154.
11 Q. Liu, Y. Yuan, J. Li, J. Liu, C. Hu, M. Chen, L. Lin, H. Kou, Y. Shi, W. Liu, H. Chen, Y. Pan, J. Guo, *Ceram. Int.*, 2014, **40(6)**, 8539−8545.
12 H. S. Jang, Y.-H. Won, D. Y. Jeon, *Appl. Phys. B*, 2009, **95(4)**, 715−720.
13 H. H. Kwak, S. J.Kim, Y. S. Park, H. H. Yoon, S. J. Park, H. W. Choi, *Mol. Cryst. Liq. Cryst.*, 2009, **513**, 106−113.C. C.
14 H. S. Jang, W. B. Im, D. C. Lee, D. Y. Jeon, S. S. Kim, *J. Lumin.*, 2007, **126**, 371−377.
15 Lin, Y. S. Zheng, H. Y. Chen, C. H. Ruan, G. W. Xiao, R. S. Liu, *J. Electrochem. Soc.*, 2010, **157(9)**, H900−H903.
16 S. Kim, T. Kim, M. Kang, S. K. Kwak, T. W. Yoo, L. S. Park, I. Yang, S. Hwang, J. E. Lee, S. K. Kim, S.-W. Kim, *J. Am. Chem. Soc.*, 2012, **134(8)**: 3804−3809.
17 Q. Zhou, Y. Y. Zhou, Y. Liu, L. J. Luo, Z. L. Wang, J. H. Peng, J. Yan, M. M. Wu, *J. Mater. Chem. C*, 2015, **3(13)**: 3055−3059.

18 W. Lü, W. Lv, Q. Zhao, M. Jiao, B. Shao, H. You, *Inorg. Chem.*, 2014, **53(22)**, 11985−11990.
19 T.-W. Kuo, W.-R. Liu, T.-M. Chen, *Opt. Express*, 2010, **18(8)**, 8187–8192.
20 J. Ruan, R.-J. Xie, N. Hirosaki, T. Takeda, *J. Am. Ceram. Soc.*, 2011, **94(2)**, 536−542.
21 S. Yamada, H. Emoto, M. Ibukiyama, N. Hirosaki, J. Eur. Ceram. Soc., 2012, **32(7)**, 1355–1358.
22 A. B. Parmentier, P. F. Smet, D. Poelman, *Opt. Mater.*, 2010, **33(2)**, 141−144.
23 S.-P. Lee, T.-S. Chan, T.-M. Chen, ACS *Appl. Mater. Interfaces*, 2015, **7(1)**, 40−44.
24 J. W. Moon, J. S. Kim, B. G. Min, H. M. Kim, J. S. Yoo, *Opt. Mater. Express*, 2014, **4(10)**, 2174−2181.
25 L.-H. Mao, Q.-H. Zhang, Y. Zhang, C.-F. Wang, S. Chen, *Ind. Eng. Chem. Res.*, 2014, **53(43)**, 16763−16770.
26 A. Aboulaich, M. Michalska, R. Schneider, A. Potdevin, J. Deschamps, R. Deloncle, G. Chadeyron, R. Mahiou, *ACS Appl. Mater. Interfaces*, 2014, 6(1), 252−258.
27 M. J. Lee, Y. H. Song, Y. L. Song, G. S. Han, H. S. Jung, D. H. Yoon, *Mater. Lett.*, 2015, **141**, 27−30.
28 P. He, H. Wang, S. Liu, J. Shi, G. Wang, M. Gong, *J. Phys. Chem. A*, 2009, **113(46)**, 12885−12890.
29 H. Wang, P. He, S. Liu, J. Shi, M. Gong, *Inorg. Chem. Commun.*, 2010, **13(1)**, 145−148.
30 G. Shao, N. Zhang, D. Lin, K. Feng, R. Cao, M. Gong, *J. Lumin.*, 2013, **138**, 195−200.
31 H. Li, R. Zhao, Y. Jia, W. Sun, J. Fu, L. Jiang, S. Zhang, R. Pang, C. Li, *ACS Appl. Mater. Interfaces*, 2014, **6(5)**, 3163−3169.
32 A. A. Setlur, R. J. Lyons, J. E. Murphy, N. P. Kumar, M. S. Kishore, *ECS J. Solid State Sci. Technol.*, 2013, **2(2)**, R3059−R3070.
33 T. Ye, S. Li, X. Wu, M. Xu, X. Wei, K. Wang, H. Bao, J. Wang, J. Chen, *J. Mater. Chem. C*, 2013, **1(28)**, 4327–4333.
34 S. Ye, F. Xiao, Y. X. Pan, Y. Y. Ma, Q. Y. Zhang, *Mater. Sci. Eng. R*, 2010, **71(1)**, 1−34.
35 N. J. Findlay, J. Bruckbauer, A. R. Inigo, B. Breig, S. Arumugam, D. J. Wallis, R. W. Martin, P. J. Skabara, *Adv. Mater.*, 2014, **26(43)**, 7290−7294.
36 H. Tang, G. Meng, Z. Chen, Y. Liu, L. Wei, Z. Wang, *J. Mater. Sci.: Mater. Electron.*, 2015, **26(5)**, 2824−2829.
37 H. Yang, G. Meng, Y. Zhou, H. Tang, J. Zhao, Z. Wang, *Materials*, 2015, **8(9)**, 6105–6116.
38 C.-Y. Sun, X.-L. Wang, X. Zhang, C. Qin, P. Li, Z.-M. Su, D.-X. Zhu, G.-G. Shan, K.-Z. Shao, H. Wu, J. Li, *Nature commun.*, 2013, **4**, 2717–1–8.
39 H. Yan, H. Wang, P. He, J. Shi, M. Gong, *Inorg. Chem. Commun.*, 2011, **14(6)**, 1065−1068.
40 J.-Y. Jin, Y.-M. Kim, S.-H. Lee, Y.-S. Lee, *Synth. Met.*, 2009, **159(17−18)**, 1804−1808.
41 J.-Y. Jin, H.-G. Kim, C.-H. Hong, E.-K. Suh, Y.-S. Lee, *Synth. Met.*, 2007, **157(2−3)**, 138−141.
42 D. D. Martino, L. Beverina, M. Sassi, S. Brovelli, R. Tubino, F. Meinardi, *Sci. Rep.-UK*, 2014, **4**, 4400−1−5.
43 R. D. Costa, E. Ortí, H. J. Bolink, F. Monti, G. Accorsi, N. Armaroli, *Angew. Chem. Int. Ed.*, 2012, **51(33)**, 8178−8211.
44 T. Hu, L. He, L. Duan, Yong Qiu, *J. Mater. Chem.*, 2012, **22(10)**, 4206−4215.
45 H. Tang, Y. Li, Q. Chen, B. Chen, Q. Qiao, W. Yang, H. Wu, Y. Cao, *Dyes Pigments*, 2014, **100**, 79−86.
46 J. M. Fernández-Hernández, C.-H. Yang, J. I. Beltrán, V. Lemaur, F. Polo, R. Fröhlich, J. Cornil, L. De Cola, *J. Am. Chem. Soc.*, 2011, **133(27)**, 10543−10558.
47 H. Tang, Y. Li, B. Zhao, W. Yang, H. Wu, Y. Cao, *Org. Electron.*, 2012, **13(12)**, 3211−3219.
48 X. Zhao, X.-Z. Wang, X.-K. Jiang, Y.-Q. Chen, Z.-T. Li, G.-J. Chen, *J. Am. Chem. Soc.*, 2003, **125(49)**, 15128−15139.
49 W. Tian, C. Yi, B. Song, Q. Qi, W. Jiang, Y. Zheng, Z. Qi, Y. Sun, *J. Mater. Chem. C*, 2014, **2(6)**, 1104−1115.
50 X.-M. Yu, H.-S. Kwok, W.-Y. Wong, G.-J. Zhou, *Chem. Mater.*, 2006, **18(21)**, 5097−5103.
51 S. Lamansky, P. Djurovich, D. Murphy, F. Abdel-Razzaq, H.-E. Lee, C. Adachi, P. E. Burrows, S. R. Forrest, M. E. Thompson, *J. Am. Chem. Soc.*, 2001, **123(18)**, 4304–4312.
52 H. Sahoo, *J. Photochem. Photobio. C: Photochem. Rev.*, 2011, **12(1)**, 20–30.

graphical abstract

Warm white was obtained when red-emitting iridium(III) complex was added in LEDs based on blue GaN chips and YAG:Ce.